Symmetric mode resonance of bubbles attached to a rigid boundary

Edward M. B. Payne,[a] Suhith J. Illesinghe,[b] and Andrew Ooi[c]
Department of Mechanical and Manufacturing Engineering, The University of Melbourne, Parkville Melbourne, Victoria 3010, Australia

Richard Manasseh[d]
CSIRO Manufacturing and Infrastructure Technology, Energy and Thermofluids Engineering, P.O. Box 56 (Graham Road), Highett Melbourne, Victoria 3190, Australia

(Received 9 March 2005; revised 15 July 2005; accepted 12 August 2005)

Experimental results are compared with a theoretical analysis concerning wall effects on the symmetric mode resonance frequency of millimeter-sized air bubbles in water. An analytical model based on a linear coupled-oscillator approximation is used to describe the oscillations of the bubbles, while the method of images is used to model the effect of the wall. Three situations are considered: a single bubble, a group of two bubbles, and a group of three bubbles. The results show that bubbles attached to a rigid boundary have lower resonance frequencies compared to when they are in an infinite uniform liquid domain (referred to as free space). Both the experimental data and theoretical analysis show that the symmetric mode resonance frequency decreases with the number of bubbles but increases as the bubbles are moved apart. Discrepancies between theory and experiment can be explained by the fact that distortion effects due to buoyancy forces and surface tension were ignored. The data presented here are intended to guide future investigations into the resonances of larger arrays of bubbles on rigid surfaces, which may assist in surface sonochemistry, sonic cleaning, and micro-mixing applications.
 [DOI: 10.1121/1.2062268]

PACS number(s): 43.20.Ks, 43.30.Dr [AJS] Pages: 2841–2849

I. INTRODUCTION

Modeling the compressible oscillations of gas bubbles dates back to 1917 with the work of Rayleigh[1] who gave the first mathematical formulation of the dynamics of a single oscillating bubble. In the family of Rayleigh-Plesset equations the radial expansion and contraction of the bubble is given by the spherically symmetric momentum equation for the liquid only; the ideal gas law is often used to give the boundary condition at the bubble wall. Minnaert[2] independently developed a simple linear relationship for the resonance frequency of a freely pulsating spherical bubble, known as the Minnaert frequency, which was derived using an energy balance approach that inherently assumed linear behavior. Extensive work has since been done toward developing a model to describe the oscillations of multiple gas bubbles in a liquid medium,[3–11] mostly analyzing pairs of bubbles. Furthermore, many investigators have been interested in how bubbles interact with each other, and in the natural frequencies of a system of an arbitrary number of bubbles.

A coupled-oscillator model based on the self-consistent approach, such as that introduced by Tolstoy[4] and later developed by Feuillade,[12] is one way to describe the collective oscillations of bubbles. This approach inherently eliminates an inconsistency in the coupled equations owing to multiple bubble re-reflections and has been shown to qualitatively predict the acoustic pressure distribution around a bubble chain.[13,14] In his work, Feuillade[12] modeled an arbitrary number of bubbles in free space, showing how the symmetric mode (where all bubbles oscillate in phase) has a lower resonance frequency than the asymmetric modes (where some, or all of the bubbles oscillate out of phase).

Due to the complex nature of surface tension and buoyancy effects, most modeling of bubbles attached to a rigid boundary has been done numerically. A good review of bubble deformation near rigid and free boundaries is given by Blake and Gibson.[15] Other workers include Chahine,[16,17] who has used a numerical boundary element method to describe bubble collapse near a solid wall. However, in terms of the current framework, for which experimental results can be easily compared to a simple linear model, numerical calculations are not required. In this paper, therefore, an image theory approach developed by Strasberg[18] will be incorporated into Feuillade's work to model the effect of the boundary.

Strasberg performed an analysis of the effect of a nearby rigid boundary on the resonance frequency of a single spherical bubble. He showed that a bubble pulsating next to the rigid boundary is equivalent to two bubbles pulsating in phase in free space, which in this paper will be referred to as the "image effect." The result of this image effect is that bubbles next to a rigid boundary have lower resonance frequencies than the same bubbles in an unbounded domain.

[a]Electronic mail: embp@ecr.mu.oz.au
[b]Electronic mail: s.illesinghe@gmail.com
[c]Electronic mail: a.ooi@unimelb.edu.au
[d]Electronic mail: Richard.Manasseh@.csiro.au

Including this into Feuillade's model is easily done and will be shown in the following. Other work, by Howkins[19] and Blue,[20] also adopted Strasberg's image theory to try to explain their experimental findings. In their work, they experimentally measured the resonance frequency of a bubble which was actually attached to a rigid boundary, and showed that the resonance frequency was lower compared to that of an equivalent bubble in free space. However their work only considered single bubble arrangements of different bubble radii, and only n different bubble radii, where $n=2$ for Blue's work and $n=11$ for Howkins' work. This paper is intended to determine whether the image theory is applicable for larger bubble groups attached to a rigid boundary, by providing original and detailed experimental results over a range of bubble sizes.

Apart from these limited experimental and theoretical studies on the resonance frequencies of multiple bubble arrangements attached to a rigid boundary, the majority of work has been carried out for bubbles in free space. For example, lower resonance frequencies for groups of bubbles has been shown by Nicholas *et al.*[21] for bubble clouds, by Feuillade[12] for up to three bubbles, and by Manasseh *et al.*[22] for a bubble chain. Furthermore, Hsiao *et al.*[8] and Leroy *et al.*[11] experimentally showed that the symmetric mode resonance frequency for two bubbles in free space is lower than the resonance frequency of a single bubble in free space. In addition, Weston[23] and Tolstoy *et al.*[24] have modeled line and plane arrays of bubbles.

The present paper thus fills a gap in the literature, in that it is concerned theoretically, but primarily experimentally, with the symmetric mode resonance frequency of multiple bubble arrangements attached to a plate, over a range of bubble sizes. From a theoretical standpoint, the current work builds upon a simplified version of Feuillade's coupled-oscillator model, in which a mirror image of bubbles is introduced to model the presence of a rigid boundary. The resulting system of equations is reduced to an analytical expression which gives the symmetric mode natural frequency of an arrangement of up to three bubbles attached to a rigid boundary, whose spacing between bubble centers is identical. Although unequal bubble spacings are an interesting added possibility, as is the possibility of unequal bubble sizes, effects of these parameters are not considered in this paper.

Experimental results for the symmetric mode resonance frequency of different arrangements of bubbles attached to a glass plate are presented. One, two, and three bubble arrangements are considered, where in each case the system was excited by a varying frequency (chirp) signal, covering the expected resonance frequency of the given bubble arrangement. The response with and without bubbles was detected by a hydrophone, allowing the symmetric mode resonance frequency to be determined. Comparison between the theoretical natural frequency and the experimental resonance frequency can be made since for the relatively large bubble sizes involved, the resonance frequency and natural frequency are essentially the same.

For ease of experimental setup, bubbles of order millimeter size were used, with natural frequencies of the order of 1000 Hz. As a result, the acoustic wavelengths in the experimental tank were large ($\approx$1.5 m) relative to the spacing between the bubbles (which was approximately three times the equilibrium radius; a typical value being 7.5 mm). Hence the symmetric mode was preferentially excited over the asymmetric modes because a given bubble arrangement was under the same pressure field at any one point in time, albeit with slight variations in the pressure amplitude and phase.

From this work, predictions of the resonance frequencies of multiple bubbles attached to a rigid boundary will potentially help in the manufacture and operation of devices for the medical-pathology field such as those already demonstrated by Liu *et al.*[25] as well as for surface sonochemistry and sonic cleaning applications.

II. THEORY

A. Development of the model

Under adiabatic conditions, the natural frequency of a spherical, millimeter-sized, linearly oscillating bubble is given by Minnaert's equation[2]

$$\omega_0 = \frac{1}{R_0}\sqrt{\frac{3\gamma P_0}{\rho}}, \tag{1}$$

where ω_0 is the circular natural frequency, γ is the ratio of gas specific heats, P_0 is the absolute liquid pressure, ρ is the liquid density, and R_0 is the equilibrium radius of the bubble.

Feuillade's model[12] is used to describe the dynamics of an arbitrary number of bubbles located in free space, driven by an external pressure field. Mathematically this is given by the following coupled differential equation:

$$m_i\ddot{v}_i + b_i\dot{v}_i + \kappa_i v_i = -P_i e^{I(\omega t+\phi_i)} - \sum_{j\neq i}^{N}\frac{\rho}{4\pi s_{ji}}\ddot{v}_j(t - s_{ij}/c), \tag{2}$$

where v_i represents the differential volume of the ith bubble (i.e., the difference between the instantaneous and equilibrium bubble volumes), $m_i(=\rho/4\pi R_{0_i})$ is the inertial "mass" of bubble i, having radius R_{0_i}, b_i describes the damping, and $\kappa_i(=3\gamma P_0/4\pi R_{0_i}^3)$ is the "adiabatic stiffness." The amplitude and phase of the external field experienced by the ith bubble are denoted by P_i and ϕ_i, respectively, and s_{ji} denotes the center-to-center distance between bubbles i and j. The angular driving frequency is denoted by ω and t is time. The imaginary unit is denoted by I. The last term on the right-hand side describes the time delay coupling between the bubbles due to their oscillating pressure fields. The speed of sound in water is denoted by c.

Since only the natural frequencies are required, the external field acting on each bubble is neglected. Later it will be shown that the natural frequency is a very close approximation to the resonance frequency, given the relatively large bubble sizes considered. The time delay in the second term on the right-hand side of Eq. (2) can be neglected since there is negligible time for the sound to propagate from one bubble to another. In other words, because of the small bubble separations considered (e.g., $s_{ij}=7.5$ mm) and the relative speed of sound in water (i.e., $c=1480$ m/s), the time delay term $s_{ij}/c \approx 5\times10^{-6}$ s and will be assumed to be small enough,

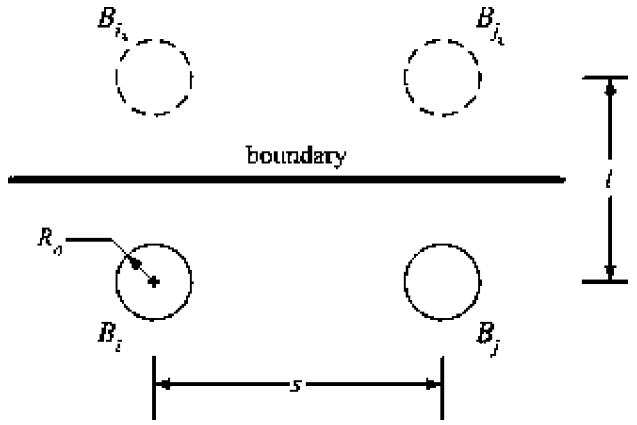

FIG. 1. Schematic of bubble image model for $N=2$. The solid line represents the real bubble and the dashed line represents the image bubble.

compared to the natural period of an oscillating bubble, to neglect. Further, it has been shown by Doinikov *et al.*[14] that time delays only affect the damping but not the natural frequencies of the natural modes of the system when the bubbles are not too far apart. Since the interest of this paper is only on the natural frequencies of the system, it is anticipated that neglecting time delays will not affect any of the data presented in this paper. As a further simplification it is assumed that the bubbles have identical radii and the same physical properties (i.e., $R_{0_1}=R_{0_2}=\ldots=R_{0_N}=R_0$, $m_1=m_2=\ldots=m_N=m$, etc.). Therefore Eq. (2) reduces to

$$m\ddot{v}_i + b\dot{v}_i + \kappa v_i = -\sum_{j\neq i}^{N} \frac{\rho}{4\pi s_{ji}}\ddot{v}_j. \tag{3}$$

It can be seen that the solution of the above gives N different eigenmodes each having an associated eigenfrequency.

B. Introduction of a rigid boundary

Consider the dynamics of a planar array of bubbles situated a distance $l/2$ from a rigid boundary. A bubble next to a rigid boundary creates an acoustic image of itself,[12] which oscillates in phase with the original bubble and is coupled to it. Under the above-mentioned assumptions, the bubble produces a velocity field like a potential-flow source or sink; hence the rigid boundary can be modeled by a mirror image. This is depicted in Fig. 1 for the simple case of two bubbles B_i and B_j. Note that $l(=s_{ii_\iota})$ is the separation between a bubble and its image (e.g., B_i and B_{i_ι}).

It can be seen by examining Eq. (3) with j set to i_ι that the image bubble (which simulates the solid wall) has the effect of increasing the effective mass on the real bubble. Physically this is because the boundary forces the streamlines to be parallel to itself and hence into a new (more constrained) topology. Thus, an extra term (given by R_0/l) arises as part of the inertial coefficient for bubble i. Also an extra term (given by $\rho/4\pi l_{j_\iota i}$) arises because of the coupling between a given bubble i and all the other bubble images j_ι. Equation (3) thus becomes

$$\left(m + m\frac{R_0}{l}\right)\ddot{v}_i + b\dot{v}_i + \kappa v_i = -\sum_{j\neq i}^{N}\left(\frac{\rho}{4\pi s_{ji}} + \frac{\rho}{4\pi l_{j_\iota i}}\right)\ddot{v}_j, \tag{4}$$

where $l_{j_\iota i}(=\overline{s^2+l^2})$ denotes the radial distance between image bubble j_ι and bubble i.

An analytical expression is obtained for the undamped natural symmetric mode frequency for $N\leqslant 3$ bubbles,[26] in which the separation between bubble centers, s, is identical. Since the symmetric mode is assumed all bubbles pulsate with the same amplitude and phase, it follows that for the undamped case, Eq. (4) reduces to one independent equation given by

$$\left(m + m\frac{R_0}{l}\right)\ddot{v} + \kappa v = -(N-1)\frac{\rho}{4\pi}\left(\frac{1}{s} + \frac{1}{l_\iota}\right)\ddot{v}, \tag{5}$$

where $l_\iota = \overline{s^2+l^2}$. Grouping inertia terms, dividing through by m and noting that $m=\rho/(4\pi R_0)$ and $\kappa/m=3\gamma P_0/(\rho R_0^2)=\omega_0^2$, yields

$$\left(1 + \frac{R_0}{l} + (N-1)R_0\left(\frac{1}{s} + \frac{1}{l_\iota}\right)\right)\ddot{v} + \omega_0^2 v = 0. \tag{6}$$

The damping term has been neglected because Strasberg[18] showed that its impact on the resonance frequency is negligible for relatively large bubbles. However, it does influence the resonance frequency of small (submicron radii) bubbles, as shown by Khismatullin.[27] The natural frequency (in rad/s) of Eq. (6) is thus given by

$$\omega_{\mathrm{sym}_N} = \frac{\omega_0}{\sqrt{1 + \frac{R_0}{l} + (N-1)R_0\left(\frac{1}{s} + \frac{1}{l_\iota}\right)}}, \tag{7}$$

which holds for $N\leqslant 3$. This limitation arises because it has been assumed that the separation between bubble centers is identical and a group of three bubbles is the largest number of bubbles which satisfies the condition for a planar array. Note that $N=3$ corresponds to a group of three bubbles arranged in an equilateral triangle.

A justification for the comparison between the resonance frequency of the bubbles in the experiments and the natural frequency given by Eq. (7) is as follows. The resonance frequency is identical to the natural frequency when there is no damping. Since the bubbles considered in this paper are quite large, damping is small, meaning that the resonance frequency can be very closely approximated by the undamped natural frequency given by Eq. (7). To show this, a plot of the amplitude response (in terms of a change in radius) of a group of two bubbles attached to a rigid boundary and driven by an external source is given in Fig. 2, where $R_0=2.5$ mm, $s=5R_0$, and $l=2R_0$. In this numerical example, the bubbles have been driven in phase (to excite the symmetric mode), and damping has been included. The amplitude has been divided by the driving amplitude to give a normalized response amplitude and is denoted by the solid line in Fig. 2. The dashed line highlights the undamped natural frequency as calculated using Eq. (7). Clearly the difference between the undamped natural frequency and the resonance frequency

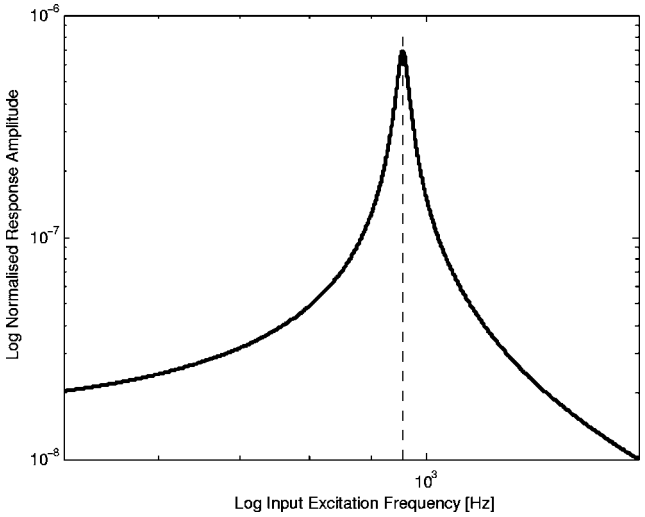

FIG. 2. Resonance frequency compared to the undamped natural frequency for a group of two bubbles attached to a rigid boundary, each with $R_0 = 2.5$ mm. Separation distance $s = 5R_0$ and $l = 2R_0$. Equation (7) is used to calculate the undamped natural frequency which is highlighted by the dashed vertical line. The resonance frequency coincides with the undamped natural frequency at approximately 956 Hz.

(the frequency at which maximum amplitude occurs) is negligible. For this example resonance occurs at approximately 956 Hz.

Bubbles are considered "attached" to the boundary when $l = 2R_0$ (the smallest physical value for l), such that the perpendicular distance from the center of a bubble to the plate is equal to R_0. Equation (7) does not allow for divergence from sphericity due to the flattening of the buoyant bubble, which in the experiment was trapped under a rigid boundary. It is therefore expected that the expression will be more valid for smaller bubbles which are closer to spherical shape. For larger bubbles however there is a significant contact area between the bubble and the boundary, resulting in reduced bubble-wall velocity near the boundary as the bubble pulsates. In this situation the image theory is no longer appropriate. Instead, the dynamics of larger bubbles are better described by hemispheres or domes as previously investigated by Blue.[20]

To do this, a hemispherical shape is assumed, equivalent in volume to half a spherical bubble. Therefore, in determining the resonance frequency of a hemispherical bubble, the radius of a spherical bubble with twice the volume of the hemispherical bubble is calculated and substituted into Minnaert's equation [Eq. (1)]. This has the effect of reducing the resonance frequency by a factor of $2^{-(1/3)}$ compared to that of a spherical bubble with the same volume as the hemisphere. It is therefore suggested that the dynamics of a large (approximately hemispherical) bubble which is attached to a boundary is equivalent to the dynamics of a single bubble (with twice the volume) pulsating in free space. This is what was implied from Blue's work. In the absence of surface tension and friction, this seems a reasonable approximation.

The above-noted consideration, which is consistent with the work of Strasberg, Blue, and Howkins, means that the resonance frequency of a bubble attached to a rigid boundary will be lower than that of a bubble with the same size in free space. But due to nonsphericity of the bubbles the resonance frequency will be slightly increased.

III. EXPERIMENT

Experiments were carried out to detect the response of air bubbles in water trapped under a glass plate when driven by an acoustic pressure field, as depicted in Fig. 3. The tank was made from 12-mm-thick Perspex with a 300 mm square base. The glass plate (of thickness 3 mm) was securely maintained at a height of 20 mm above the face of a piston which was attached to a modified speaker. A circular hole in the bottom of the tank allowed direct transfer of sound from the speaker to the water, thereby setting up an acoustic pressure field within the tank. Adhesive tape was used to seal the area adjoining the water and the face of the piston.

Air bubbles were generated with a syringe (50 μl, ALLTECH Associates Australia) with a volumetric accuracy of ±5% and were arranged as close to the center-line of the piston as possible (±0.25 mm) so as to receive maximum power from the speaker. A chirp signal was used to excite the bubbles which was preamplified before passing through the speaker. In the first set of single bubble experiments, a chirp signal of 80 ms was used, while for the second set of single bubble experiments, as well as for the two and three bubble experiments, a chirp signal of 180 ms was used. The difference in chirp duration for the two sets of single bubble ex-

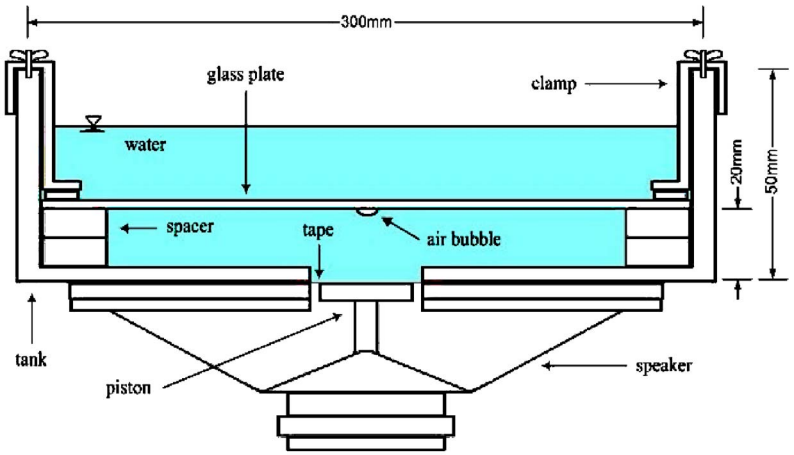

FIG. 3. (Color online) Schematic cross-sectional view of the main experimental apparatus with a single air bubble. The bubble is excited by the speaker.

TABLE I. Experimental parameters and conditions.

Density of water	1000 kg/m^3
Temperature of water	20°C
Equilibrium water pressure	10^5 Pa
Speaker driving pressure amplitudes	$<$100 Pa
Frequency range	400–3000 Hz
Polytropic index	1.33

periments is shown not to affect the resonance frequency. The applied sound pressures directly above the piston near the glass plate were typically of the order of 100 Pa or less, so as to remain in the linear regime. Frequencies employed were mostly in the 400–3000 Hz range. Table I gives a summary of the experimental conditions and parameters.

The small pressure fluctuation caused by the response of the bubbles was detected by a hydrophone (Brüel & Kjaer 8103, 9.5 mm diameter and 50 mm in length, with an essentially constant frequency response from 0.1 Hz to 20 kHz). The distance from the hydrophone's acoustic center to the closest bubble wall was approximately 7 mm. The output of the hydrophone was then fed into a charge amplifier (Brüel & Kjaer type 2634, with an essentially constant frequency response from 1 Hz to 20 kHz), and connected to a digital oscilloscope (HP54600A) for data acquisition and storage on a PC. A schematic of the setup is given in Fig. 4.

Thirty time-domain responses were captured for a given bubble volume and arrangement, and each one converted to a frequency-domain response. Likewise, 30 responses without bubbles were captured, thus measuring the response of the tank and speaker assembly only. The difference in the frequency-domain responses at each frequency with and without bubbles was scaled by dividing by the average response with no bubbles present. If the maximum "scaled" difference in power was statistically significant, the frequency at which this difference occurred was considered to be the resonance frequency of the bubble arrangement. A sample time-domain and corresponding frequency-domain response are shown in Figs. 5 and 6, respectively, for a 45 μl bubble. In Fig. 6 the maximum scaled difference occurs at around 1100 Hz, indicating that that is the resonance frequency of the bubble, when attached to the glass plate.

Although the dominant response detected by the hydrophone was believed to be pressure fluctuations caused by the radial pulsation of the bubble (the breathing mode), there was the possibility that surface modes[28] would interfere with the response. Surface modes were visually observed, but only when the system was driven at very high amplitudes. At the amplitudes used during experimentation, surface modes were not observed. Given the relatively large size of the hydrophone head compared to the small scale pressure variations caused by surface modes, any surface modes that were present would have had little influence on the hydrophone. Therefore it is quite reasonable to assume that the above-determined resonances were indeed associated with the radial pulsation of the bubble.

It should be emphasized that the purpose of this paper is to investigate the symmetric mode resonance frequency of the bubble groups, and not the other possible modes (e.g., the asymmetric mode). While the experiments were intended to excite the symmetric mode, small differences in the pressure amplitude applied to each bubble, as well as slight phase

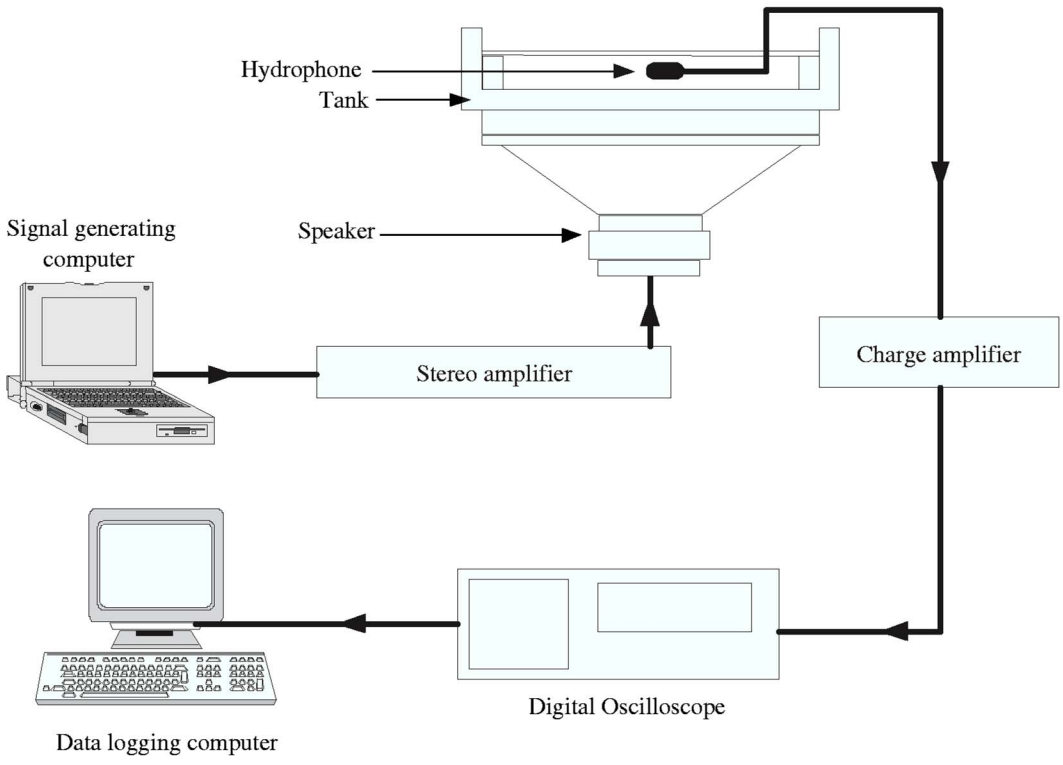

FIG. 4. (Color online) Schematic of the experimental setup. See Table I for experimental conditions.

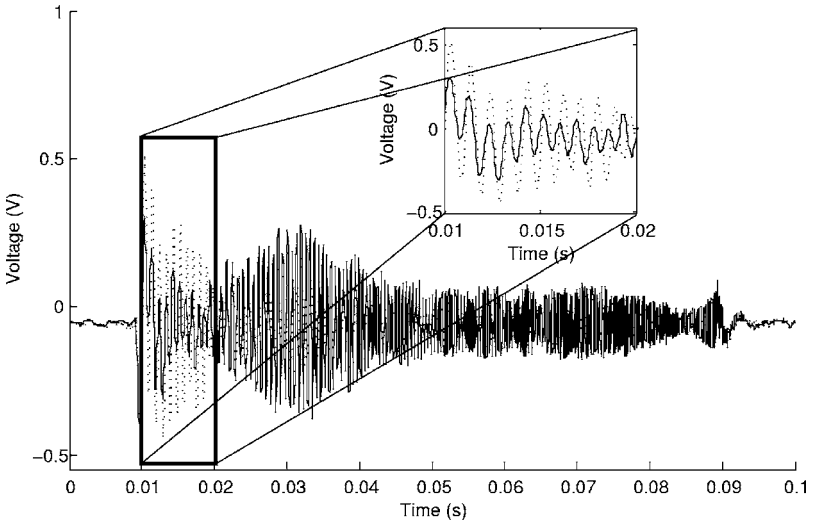

FIG. 5. Time-domain response of the system with and without bubbles. The dotted line denotes the response with a 45 μl bubble. The solid line represents the case when the bubble was removed. This test used an 80 ms chirp signal sweeping from 900 to 3500 Hz. A enlarged region from 0.01 to 0.02 s is highlighted to distinguish the response with a bubble from the response without a bubble.

differences, tended to excite asymmetric modes as well. However the symmetric mode appeared to be dominant for most of the conditions investigated. In the conditions where this was not the case, only the contribution of the symmetric mode was identified. Investigation of the asymmetric modes is beyond the scope of this paper and will be the focus of future work.

IV. RESULTS AND DISCUSSION

A. Single bubble arrangement with varying bubble size

Figure 7 shows the symmetric mode resonance frequency versus bubble radius for the case of a single bubble attached to the glass plate. Superimposed is Minnaert's relationship and the analytical expression from Eq. (7) for $N=1$, as well as the half-bubble approximation. Clearly the image theory (the analytical expression) gives a better agreement to the experimental data than Minnaert's relationship. The error bars on the experimental results are included, but are barely visible due to the tight confidence limits on the results. The radii given on the horizontal axis represent the radius of a spherical bubble with a volume (V_{inj}) equal to the bubble which was injected (i.e., $R_0=(3V_{\text{inj}}/4\pi)^{1/3}$).

As predicted by the theory, the experimental data show that smaller bubbles have higher resonance frequencies than larger ones. This is expected and confirms that the resonance response of the bubble has been detected by the hydrophone. Also, both the image theory and the experimental data lie below Minnaert's relationship, which is consistent with the data of previous investigators;[18–20] and from the present work, enough data points are now available for the functional form of the relation to be confirmed. According to the image theory, this can be reasoned as follows. The effect of the boundary is equivalent to introducing an image bubble adjacent to the real bubble. Since the image bubble will exactly "mirror" the real bubble, there is a symmetric coupling between the real bubble and the image bubble. This increases the effective mass of the system, resulting in a decrease in

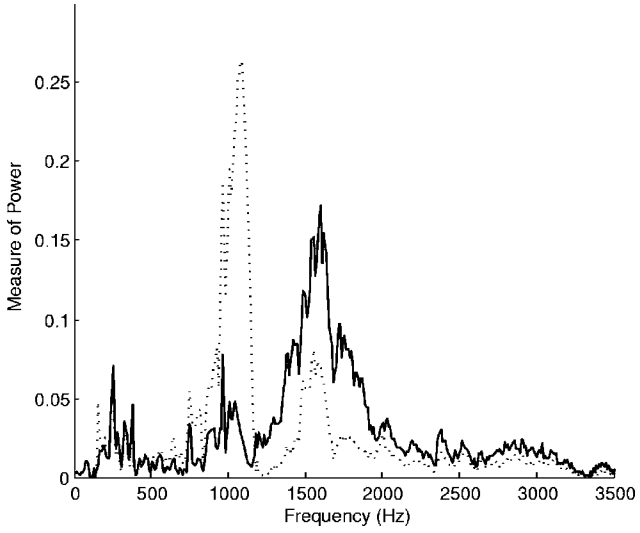

FIG. 6. Frequency-domain response of the system with and without bubbles. The dotted line denotes the response with a 45 μl bubble. The solid line represents the case when the bubble was removed.

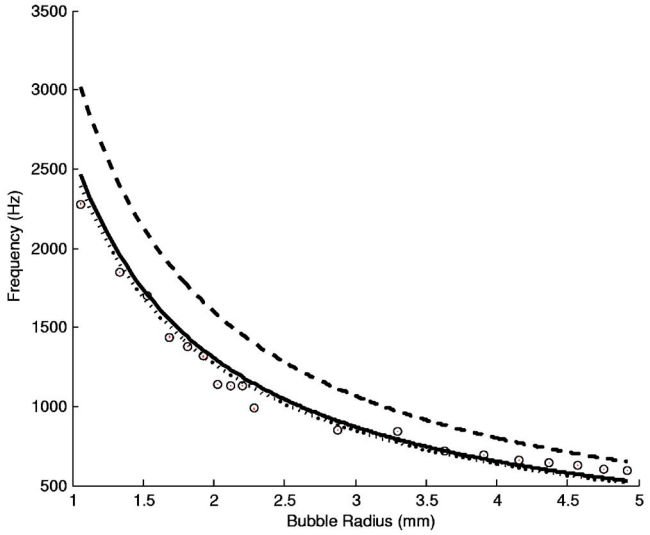

FIG. 7. Comparison of experimental resonance frequencies and theoretical undamped natural frequencies for a single bubble of varying radius. (---) Minnaert's equation and (—) represents the analytical expression for $N=1$. (···) The half-bubble approximation. The points denoted ◯ are the experimental results, with error bars shown by vertical lines.

resonance frequency. This is analogous to a mass-spring system where an increase in the mass will lower the resonance frequency.

Although a bubble (especially a large bubble) is flattened when attached to a plate (due to buoyancy and surface tension) the deviation from spherical shape does not appear to greatly affect the resonance frequency. Strasberg's work on the resonance frequency of oblate spheroids is consistent with this observation. In his work, he showed that as a bubble is deformed from sphericity its pulsation frequency increases, but slightly, increasing by only 2% when the bubble becomes a spheroid with a ratio of major to minor axes equal to 2 (see Table I of Strasberg's work[18]). Admittedly, his work was for a bubble in free space, but it appears to be consistent with the trend observed in our experimental data.

For small bubbles the experimental data show close agreement with the analytical expression, but on closer analysis (for radii less than about 3 mm) there is a slight downwards shift in the experimental data. A possible explanation for this is as follows. Recall that the analytical expression was based on the assumption that the bubble is spherical and is just touching the boundary, meaning that distance between the real bubble and its image is given by $l=2R_0$. However, even the smallest bubbles used in the experiments were slightly flattened, giving $l<2R_0$. This increases the effective mass and hence decreases the resonance frequency. Consequently the experimental data points are lower than the analytical expression. There may be other reasons for the slight downwards shift; such as damping effects. It is known from elementary mechanics that the damped resonance frequency of a simple harmonic oscillator (such as a bubble) is lower than the damped natural frequency. The fact that there is a downwards shift for smaller bubbles is consistent with damping having a greater influence on the resonance frequency of smaller bubbles, as proposed by Khismatullin.[27]

The upwards shift in experimental data points from the image theory for larger bubble radii (>3 mm) is not as clearly justified. The measured eccentricity of the spheroidal-shaped bubbles used in the experiments was approximately equal to 2, and so the increase in resonance frequency according to Strasberg's[18] work is insignificant. Furthermore, the above-mentioned flattening effect (which has a greater impact on larger bubbles), would tend to decrease the resonance frequency, making the fit even worse. Even with the half-bubble approximation, which is a worse fit than the image theory (but a more realistic physical approximation), the increase in resonance frequency caused by the flattening of the bubble would be less than 2%, hardly enough to explain the significant upward shift.

Thus, at this point there seems to be no reasonable explanation for the upwards shift in experimental data points for larger bubbles. Nonetheless, the limited results of Blue and Howkins have been found to be consistent with the present data, in that for small bubbles (which were used by Blue) the experimental data lie below both Minnaert and the image (equivalent to Strasberg's) theory, while for larger bubbles (which were used by Howkins) the experimental data lie between Minnaert and Strasberg's theory. The transition from a downwards to upwards shift in the experimental results as the bubble size increases suggests that for a bubble attached to a rigid boundary, there is a critical bubble size greater than which surface tension and buoyancy forces significantly alter the dynamics and hence resonance frequency of the system.

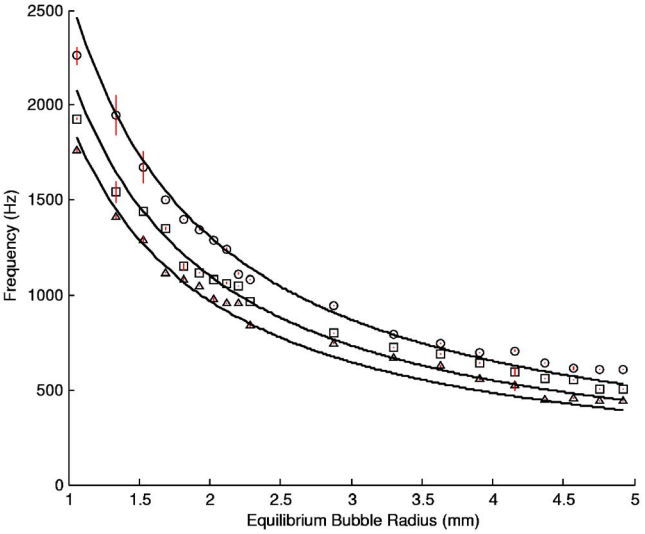

FIG. 8. (Color online) Comparison of experimental resonance frequencies and theoretical undamped natural frequencies for one, two, and three bubble arrangements vs bubble radius at a fixed separation, $s=3R_0$. (—) The analytical expression for one bubble (top curve), two bubbles (middle curve), and three bubbles (bottom curve). The points denoted ◯, □, and △ are the experimental results for one, two, and three bubbles, respectively, with error bars shown by vertical lines.

B. Multiple bubble arrangements with varying bubble size

Figure 8 shows the experimental data for a three bubble group arranged in an equilateral triangle, a two bubble group, and a single bubble. The respective analytical expressions for $N=3$, $N=2$, and $N=1$ are superimposed. For the arrangements with two and three bubbles, the separation between bubble centers was kept constant at approximately $3R_0$, in which the radius of the bubble was known from the injected volumetric measurement. Small variations in the volume of air injected to make the bubbles had negligible impact on the bubble radius (less than 1.7%).

As with the previous single bubble case, a similar trend (in terms of variation of resonance frequency with bubble size) is seen here; where for large bubble radii there is an upwards divergence from the analytical expression while for smaller bubble radii there is a downwards shift.

As evident in Fig. 8, the analytical curves are displaced downwards as N increases. This agrees with the trend in the experimental data. The downwards shift can be explained by the increase in effective mass for larger bubble groups, resulting in a lower resonance frequency. There is a clear distinction between each arrangement which is statistically significant since the error bars do not overlap for any given bubble size.

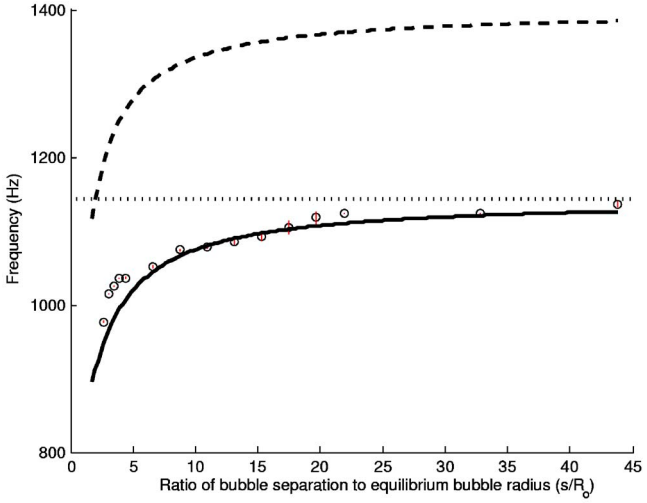

FIG. 9. (Color online) Resonance frequency vs ratio of bubble separation to bubble radius for two 50 μl bubbles (R_0=2.29 mm). (---) The undamped symmetric mode frequency for two spherical bubbles in free space. (—) The analytical expression (7) for N=2 and l=2R_0. (···) The limit as s approaches infinity. The points denoted ◯ are the experimental results, with error bars shown by vertical lines.

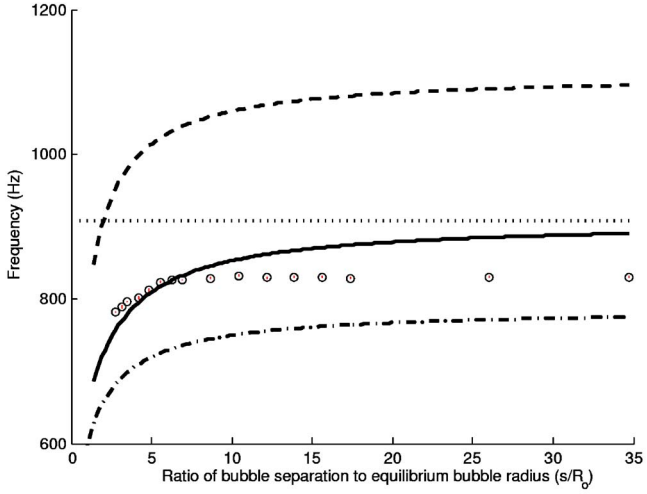

FIG. 10. (Color online) Resonance frequency vs ratio of bubble separation to bubble radius for two 100 μl bubbles (R_0=2.88 mm). (---) The undamped symmetric mode frequency for two spherical bubbles in free space. (—) The analytical expression (7) for N=2 and l=2R_0, while (–.–) represents the analytical expression for l=R_0. (···) shows the limit as s approaches infinity. The points denoted ◯ are the experimental results, with error bars shown by vertical lines.

C. Variation of resonance frequency with bubble separation

Hsiao *et al.*[8] gave experimental results for the case of two bubbles interacting in free space at varying separation. Their results agree with that predicted by their theory, showing that the symmetric mode resonance frequency decreases as the bubbles are brought closer together. However, there does not appear in the literature to be results for the case of two and three bubbles attached to a rigid boundary. Hence the purpose of the present results, which show that the same trend as documented for bubbles in free space, also holds for bubbles attached to a rigid boundary. The results also clearly show that the image theory is a much better approximation than the theory for groups of bubbles in an unbounded domain.

Figure 9 shows how the symmetric mode resonance frequency decreases as two identical 50 μl bubbles are brought closer together. The reduction in frequency for smaller separations is due to the increased effective mass on each bubble.[12] Conversely, when the bubbles are further apart, the image loading due to the interaction of the pair is weaker and the frequency approaches that of a single bubble attached to a boundary, shown by the dotted horizontal line in Fig. 9 and subsequent figures.

As mentioned, the radius of a given bubble was known from the volumetric measurement. Thus for a 50 μl bubble the nominal spherical radius is 2.29 mm. For a 100 μl bubble the radius is 2.88 mm. In order to change the ratio of bubble separation to bubble radius, s/R_0, the radii of the bubbles were kept constant while the bubble separation was varied (by moving one of the bubbles and keeping the other fixed). The analytical expression [Eq. (7)] is given by the solid line in Fig. 9. The expression for two bubbles in an unbounded domain is equivalent to setting l=∞ in Eq. (7) with N=2, resulting in the same expression given by Hsiao *et al.*[8] This is also plotted in Fig. 9 and is given by the dashed line.

Figure 10 shows the same as Fig. 9 but for two 100 μl bubbles. The same trend is observed, verifying that the results are reproducible, but there is a larger discrepancy between the experiment and theory for large values of s/R_0. Also plotted is the image theory for l=R_0, given by the dash-dot line. This has been plotted because the bubbles are squashed and the center distance to their image is less than 2R_0. On comparison with this line however, there still remains a significant discrepancy, which is possibly due to surface tension and buoyancy force effects.

The variation in symmetric mode resonance frequency with bubble separation was also performed on a group of three equi-spaced bubbles. Figure 11 shows the results for three 10 μl bubbles (nominal spherical radius of 1.34 mm). A consistent trend is observed in reasonable agreement with the theory. The fact that this trend is observed supports the assumption that the interaction between the pair of bubbles is caused by the coupled radial pulsations, rather than surface modes.

V. CONCLUSIONS

The results from this work show that bubbles attached to a rigid boundary have similar resonance trends to bubbles in free space, while the actual frequencies are lower. It has been shown theoretically and experimentally that smaller bubbles have higher resonance frequencies than larger bubbles, and that larger groups of bubbles have lower resonance frequencies than smaller groups. The deviation from sphericity was shown to have a minor effect on the frequencies predicted by the analytical expression, and is clearly less dominant than the increase in image loading caused by the decrease in separation between a real bubble and its image. Furthermore,

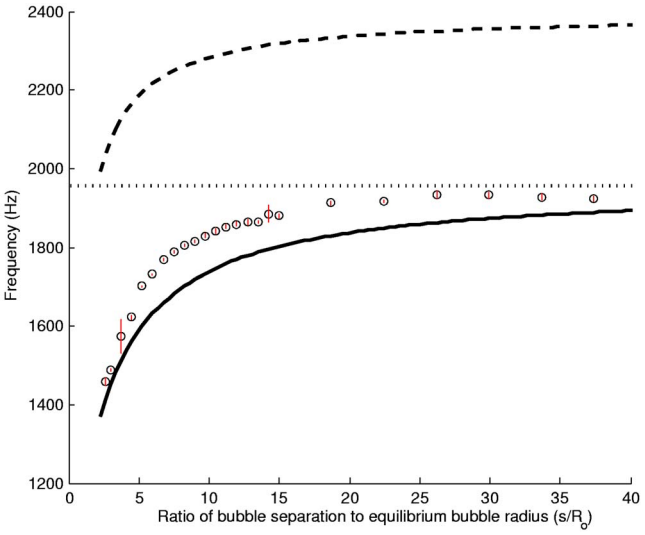

FIG. 11. (Color online) Resonance frequency vs ratio of bubble separation to bubble radius for three 10 μl bubbles (R_0=1.34 mm). (---) The undamped symmetric mode frequency for three spherical bubbles in free space. (—) The analytical expression (7) for N=3 and l=2R_0. (···) The limit as s approaches infinity. The points denoted ◯ are the experimental results, with error bars shown by vertical lines.

despite the assumptions of spherical bubble shape and the neglect of surface tension and damping, overall the analytical expression shows good agreement with the experimental results. This is a useful outcome, because it means that the resonance frequency of bubble arrays with greater number of bubbles can be predicted with a certain degree of accuracy. However, for very small bubbles, damping would have to be more rigorously considered. Future experimental work in this direction would help validate such predictions and provide guidance for the investigation of acoustic streaming from bubble arrays as well as sonic cleaning applications.

ACKNOWLEDGMENTS

The authors are very grateful to CSIRO Manufacturing & Infrastructure Technology for providing assistance throughout the experimental stage of this work. We are also appreciative of the assistance of Professor Ray Watson (Department of Mathematics and Statistics, University of Melbourne), who instructed us on the statistical analysis of the experimental results. Thanks also to Darren Waters and Nicholas Adler for their help in the design of the tank.

[1]L. Rayleigh, "On the pressure developed in a liquid during the collapse of a spherical cavity," Philos. Mag. **34**, 94–98 (1917).
[2]M. Minnaert, "On musical air bubbles and the sound of running water," Philos. Mag. **16**, 235–248 (1933).
[3]E. A. Zabolotskaya, "Interaction of gas bubbles in a sound field," Sov. Phys. Acoust. **30**, 365–368 (1984).
[4]I. Tolstoy, "Superresonant systems of scatterers. I," J. Acoust. Soc. Am. **80**, 282–294 (1986).
[5]H. Ogũz and A. Properetti, "A generalization of the impulse and virial theorems with an application to bubble oscillations," J. Fluid Mech. **218**, 143–162 (1990).
[6]A. A. Doinikov and S. T. Zavtrak, "On the mutual interation of two gas bubbles in a sound field," Phys. Fluids **7**, 1923–1930 (1995).
[7]K. Ohsaka and E. H. Trinh, "A two frequency acoustic technique for bubble resonant oscillation studies," J. Acoust. Soc. Am. **107**, 1346–1351 (2000).
[8]P. Y. Hsiao, M. Devaud, and J. Bacri, "Acoustic coupling between two air bubbles in water," Eur. Phys. J. E **4**, 5–10 (2001).
[9]M. Ida, "A characteristic frequency of two mutually interating gas bubbles in an acoustic field," Phys. Lett. A **297**, 210–217 (2002).
[10]M. Ida, "Number of transition frequencies of a system containing an arbitrary number of gas bubbles," J. Phys. Soc. Jpn. **71**, 1214–1217 (2002).
[11]V. Leroy, M. Devaud, and J. Bacri, "The air bubble: Experiments on an unusual harmonic oscillator," Am. J. Phys. **70**, 1012–1019 (2002).
[12]C. Feuillade, "Scattering from collective modes of air bubbles in water and the physical mechanism of superresonances," J. Acoust. Soc. Am. **98**, 1178–1190 (1995).
[13]R. Manasseh, A. Nikolovska, A. Ooi, and S. Yoshida, "Anisotropy in the sound field generated by a bubble chain," J. Sound Vib. **278**, 807–823 (2004).
[14]A. A. Doinikov, R. Manasseh, and A. Ooi, "Time delays in coupled multibubble systems," J. Acoust. Soc. Am. **116**, 1–4 (2005).
[15]J. R. Blake and D. C. Gibson, "Cavitation bubbles near boundaries," Annu. Rev. Fluid Mech. **19**, 99–123 (1987).
[16]G. L. Chahine, "Experimental and asymptotic study of non-spherical bubble collapse," Appl. Sci. Res. **38**, 187–197 (1982).
[17]G. L. Chahine, "Cavitation dynamics at microscale level," J. Heart Valve Dis. **3**, 102–116 (1994).
[18]M. Strasberg, "The pulsation frequency of nonspherical gas bubbles in liquids," J. Acoust. Soc. Am. **25**, 536–537 (1953).
[19]S. D. Howkins, "Measurements of the resonant frequency of a bubble near a rigid boundary," J. Acoust. Soc. Am. **37**, 504–508 (1965).
[20]J. E. Blue, "Resonance of a bubble on an infinite rigid boundary," J. Acoust. Soc. Am. **41**, 369–372 (1967).
[21]M. Nicholas, R. A. Roy, and L. A. Crum, "Sound emissions by a laboratory bubble cloud," J. Acoust. Soc. Am. **95**, 3171–3181 (1994).
[22]R. Manasseh, R. F. LaFontaine, J. Davy, I. C. Shepherd, and Y. Zhu, "Passive acoustic bubble sizing in sparged systems," Exp. Fluids **30**, 672–682 (2001).
[23]D. F. Weston, "Acoustic interaction effects in arrays of small spheres," J. Acoust. Soc. Am. **39**, 316–322 (1966).
[24]I. Tolstoy and A. Tolstoy, "Line and plane arrays of resonant monopole scatterers," J. Acoust. Soc. Am. **87**, 1038–1043 (1990).
[25]R. H. Liu, J. Yang, M. Z. Pindera, M. Athavale, and P. Grodzinski, "Bubble-induced acoustic micromixing," Lab Chip **2**, 151–157 (2002).
[26]A. Ooi and R. Manasseh, "Coupled nonlinear oscillations of microbubbles," Aust N. Z. Ind. Appl. Math. J. **46**, C102–C116 (2005).
[27]D. B. Khismatullin, "Resonance frequency of microbubbles: Effect of viscosity," J. Acoust. Soc. Am. **116**, 1463–1473 (2004).
[28]H. Lamb, *Hydrodynamics* (Cambridge University Press, Cambridge, 1997).